



Published in final edited form as:

*Endocr Relat Cancer*. 2017 November ; 24(11): L79–L82. doi:10.1530/ERC-17-0359.

## Molecular and phenotypic evaluation of a novel germline *TMEM127* mutation with an uncommon clinical presentation

Yilun Deng<sup>1</sup>, Shahida K. Flores<sup>1</sup>, ZiMing Cheng<sup>1</sup>, Yuejuan Qin<sup>1</sup>, Robin C. Schwartz<sup>2,3</sup>, Carl Malchoff<sup>3</sup>, and Patricia L. M. Dahia<sup>1</sup>

<sup>1</sup>Division of Hematology and Medical Oncology, Dept. Medicine, Cancer Therapy and Research Center, University of Texas Health Science Center at San Antonio (UTHSCSA), San Antonio, TX

<sup>2</sup>Dept. of Genetics and Genome Sciences, UCONN Health

<sup>3</sup>University of Connecticut Carole and Ray Neag Comprehensive Cancer Center

### Dear Editor

Germline mutations of the endomembrane-encoding gene *TMEM127* confers susceptibility to neural crest-derived tumors pheochromocytomas (PHEOs)(Qin, et al. 2010) and have also been found in isolated renal cell carcinomas (RCCs)(Qin, et al. 2014). PHEOs and RCCs can arise as a result of inherited susceptibility, as in in von Hippel Lindau disease and in PHEO-paraganglioma syndromes related to mutations in succinate dehydrogenase (*SDH*) subunit genes(Dahia 2014; Maher 2011). The clinical spectrum and the signaling consequences of *TMEM127* mutations remain poorly defined and it is not clear whether both tumors can be associated in families. This information would have an impact on surveillance and management of *TMEM127* mutation carriers. Here we report the investigation of a *TMEM127* mutation detected in a patient with both PHEO and RCC.

A female patient was diagnosed with a 3cm, right adrenal, metanephrine-secreting (PHEO) at age 47, and 11 years later, developed a Furhman grade I-II RCC with typical features of clear cell type. She remains disease-free after 18 and 7 years of follow up, respectively. She had two siblings with PHEOs, detected at 44 and 51 years of age, but no other RCCs. A germline truncating *TMEM127* mutation, c.532\_533dupT; p.Y178LfsX48, hereafter referred to as *TMEM127-532dupT*, was identified after a targeted, exome-based next generation sequencing screening (Fig.1C). No other pathogenic germline mutation was detected in other 35 pheochromocytoma and/or renal cancer susceptibility genes screened. Furthermore, no somatic mutations were found at high-depth sequencing (average 180x) of the proband's frozen PHEO using Illumina TruSeq Cancer Panel screening of 42 cancer genes. The *TMEM127-532dupT* mutation was also detected in germline DNA from one affected sister

### Contributions

P.L.M.D. supervised the entire study and research. Y.D., S.K.F and P.L.M.D. designed the research, analyzed and interpreted data, and wrote the manuscript. Y.D., S.K.F, Z-M.C., and Y.Q. performed all the laboratory experiments. R.S. and C.M. performed genetic counseling and clinical activities, respectively. All authors reviewed/edited the manuscript.

### Declaration of interest

The authors declare that there is no conflict of interest that could be perceived as prejudicing the impartiality of the research reported.

(Fig.1A, 1B) and three other family members, their mother and two brothers, who have no evidence of PHEO or RCC (Fig. 1A). The proband's mother was diagnosed with a lung adenocarcinoma at age 78. Analysis of the proband's fresh-frozen PHEO DNA revealed loss of the wild-type *TMEM127* allele (Fig.1B). These results support the germline *TMEM127* mutation as the main driver event in this family (Qin et al. 2010). In contrast, no *TMEM127* loss was found in three separate regions dissected from the proband's formalin-fixed paraffin embedded (FFPE) RCC (Fig.1C). Similar to the proband's PHEO, the FFPE PHEO from the proband's sister displayed clear loss of heterozygosity (LOH) of the wild-type allele (Fig. 1C), excluding potential artifacts due to fixed tissue quality. The lack of *TMEM127* LOH in the RCC is in agreement with our earlier observation of retention of heterozygosity in a limited set of renal cancers with germline *TMEM127* mutations (Qin et al. 2014). Interestingly, in this earlier report we noted decreased *TMEM127* transcription in the tumors carrying these heterozygous variants, potentially suggesting a dosage effect of the *TMEM127* mutation in renal tissue.

To further investigate whether the *TMEM127-532dupT* mutation was pathogenic, we explored its consequences in tumor tissue. No frozen material was available from the RCC and, in the absence of a reliable *TMEM127* antibody for immunohistochemistry, no additional analysis of *TMEM127* protein was available from this tumor. However, Western blot of protein lysates from the proband's frozen PHEO using a polyclonal antibody that recognizes the *TMEM127* N-terminus (Bethyl labs) (Qin et al. 2014) revealed neither full-length nor truncated *TMEM127* bands (Fig 1D). Other *TMEM127*-mutant PHEOs included as controls also showed no *TMEM127* expression, while *TMEM127* protein was clearly detectable in PHEOs of other genetic origins but with intact *TMEM127* sequence (Fig.1D), in support of instability of mutant *TMEM127* protein. In addition, in agreement with our previous observations suggesting that the mTORC1 kinase pathway is activated after *TMEM127* loss (Qin et al. 2010), phosphorylation of the mTORC1 downstream target S6 kinase (S6K) was increased in the *TMEM127-532dupT* PHEO and in the other *TMEM127* mutant tumors, compared to *TMEM127* wild-type PHEOs (Fig.1D).

Next, we examined *TMEM127* subcellular distribution as another functional readout by expressing in HEK293T kidney cells a construct carrying this mutation fused with a green fluorescent protein (GFP) made by site directed mutagenesis, as described (Qin et al. 2010). The *TMEM127-532dupT* mutant showed a diffuse cytoplasmic pattern, similar to a previously reported pathogenic *TMEM127* mutant (Qin et al. 2014), but distinct from the punctate endomembrane distribution of wild type *TMEM127* (Fig.1E). We were unable to generate cells that retained stable expression of this mutant, further supporting its instability. To study the effects of the mutation in a more physiological context in renal cells, we generated HEK293 cells carrying homozygous *TMEM127-532dupT* mutation by CRISPR-Cas9-based genome modification using previously published protocols (Sanjana, et al. 2014) and a guide RNA that targeted the mutated nucleotide site or a control (Fig.1F). Stable clones carrying the c.532dupT mutation in homozygosity were obtained and verified by sequencing (Fig 1F). Similar to the proband's PHEO, HEK293 *TMEM127-532dupT* cells had no detectable *TMEM127* protein (Fig1G). Moreover, incubation of these cells with amino acids following 2 hours of amino acid deprivation, a powerful mTORC1 pathway activation input (Sancak, et al. 2010), led to higher mTOR target phosphorylation in HEK293

TMEM127-532dupT cells compared with control (Fig. 1G), suggesting that kidney cells with mutant TMEM127-532dupT have increased mTORC1 activation. Taken together, our data indicate that the TMEM127-532dupT mutation leads to loss of TMEM127 function both in primary PHEO and in renal cells, consistent with its pathogenic role.

In view of the lack of TMEM127 LOH in the RCC, we investigated other possible genetic causes. Immunohistochemistry for SDHB was positive, excluding an SDH mutation. We sequenced the coding region of the *VHL* gene in three subsections of proband's RCC and found no mutations. We also evaluated *VHL* copy number using a SNP located in the 3'UTR of the gene (dbSNP rs1642742, c.\*294G>A) that was heterozygous in the proband germline (Fig. 1H). The three RCC regions showed variable imbalance of one allele (A; 36±6.1%), which was not detected in either of the PHEOs (~50%, Fig. 1H). This finding is consistent with partial loss of one *VHL* allele in the RCC. *VHL* disruptions are the most frequent genetic event in sporadic kidney cancers and are usually biallelic (TCGA 2013). The partial *VHL* loss in our patient's RCC suggests possible *VHL* involvement in this tumor, although we could not detect a second inactivating hit in the retained *VHL* allele. In addition, we cannot exclude that the partial *VHL* loss is a secondary, rather than an initiating, event in this tumor. Additional experiments (e.g. *VHL* promoter methylation) were limited by the lack of RCC tissue availability.

Taken together, our results establish the pathogenic nature of the *TMEM127-532dupT* mutation as the primary cause of PHEO, but do not conclusively link *TMEM127* with the RCC in this family. However, it is not possible to completely exclude *TMEM127*'s contribution to the RCC. First, the late disease onset in this family could indicate that other mutation carriers may still develop the disease. Secondly, lack of LOH in previously reported RCCs with *TMEM127* mutation (Qin et al. 2014) may point to different mechanisms of *TMEM127* inactivation in the kidney or a haploinsufficiency effect. Finally, other cases of co-existence of PHEO and RCC were recently reported in the context of *TMEM127* variants. One report described a patient with PHEO and clear cell RCC carrying a truncating germline *TMEM127* mutation; however no information is available on the LOH status or somatic sequence profile of this tumor (Hernandez, et al. 2015). In a separate article, two patients presenting with paraganglioma associated with renal tumors, one with multiple papillary adenomas and another with clear cell RCC, had novel *TMEM127* variants which target a conserved residue previously reported in a patient with PHEO (Gupta, et al. 2017). In summary, the rare co-occurrences of RCC and PHEO in *TMEM127* mutant carriers may be simply coincidental and the RCC may be sporadic in these cases. However, the caveats discussed above and the increasing number of susceptibility genes common to both PHEOs and RCCs (Dahia 2014) justify augmented awareness and long-term follow up of *TMEM127* mutation carriers in these families to conclusively establish whether their risk for RCCs is increased.

## Acknowledgments

The authors are grateful to members of the Familial Pheochromocytoma Consortium for their continuing collaboration, and patients and their families for their invaluable contributions. This work was supported by the Cancer Prevention and Research Institute of Texas (CPRIT) Individual Investigator Grants RP101202 and RP57154 (P.L.M.D), CPRIT Training Grant RP140105 (Y.D.); NRSA Institutional Predoctoral Training Grant T32CA148724

(S.K.F.); NIH-GM114102 (P.L.M.D.); Department of Defense CDMRP W81XWH-12-1-0508 (P.L.M.D.). The Optical Imaging Core Facility is supported by NIH-NCI P30-CA54174 (CTRC at UTHSCSA) and NIH-NIA P01-AG19316.

## References

- Dahia PL. Pheochromocytoma and paraganglioma pathogenesis: learning from genetic heterogeneity. *Nat Rev Cancer*. 2014; 14:108–119. [PubMed: 24442145]
- Gupta S, Zhang J, Milosevic D, Mills JR, Grebe SK, Smith SC, Erickson LA. Primary Renal Paragangliomas and Renal Neoplasia Associated with Pheochromocytoma/Paraganglioma: Analysis of von Hippel-Lindau (VHL), Succinate Dehydrogenase (SDHX) and Transmembrane Protein 127 (TMEM127). *Endocr Pathol*. 2017; Epub 06/25/2017. doi: 10.1007/s12022-017-9489-0
- Hernandez KG, Ezzat S, Morel CF, Swallow C, Otremba M, Dickson BC, Asa SL, Mete O. Familial pheochromocytoma and renal cell carcinoma syndrome: TMEM127 as a novel candidate gene for the association. *Virchows Arch*. 2015; 466:727–732. [PubMed: 25800244]
- Maher ER. Genetics of familial renal cancers. *Nephron Exp Nephrol*. 2011; 118:e21–26. [PubMed: 21071978]
- Qin Y, Deng Y, Ricketts CJ, Srikantan S, Wang E, Maher ER, Dahia PL. The tumor susceptibility gene TMEM127 is mutated in renal cell carcinomas and modulates endolysosomal function. *Hum Mol Genet*. 2014; 23:2428–2439. [PubMed: 24334765]
- Qin Y, Yao L, King EE, Buddavarapu K, Lenci RE, Chocron ES, Lechleiter JD, Sass M, Aronin N, Schiavi F, et al. Germline mutations in TMEM127 confer susceptibility to pheochromocytoma. *Nat Genet*. 2010; 42:229–233. [PubMed: 20154675]
- Sancak Y, Bar-Peled L, Zoncu R, Markhard AL, Nada S, Sabatini DM. Ragulator-Rag complex targets mTORC1 to the lysosomal surface and is necessary for its activation by amino acids. *Cell*. 2010; 141:290–303. [PubMed: 20381137]
- Sanjana NE, Shalem O, Zhang F. Improved vectors and genome-wide libraries for CRISPR screening. *Nat Methods*. 2014; 11:783–784. [PubMed: 25075903]
- TCGA. Comprehensive molecular characterization of clear cell renal cell carcinoma. *Nature*. 2013; 499:43–49. [PubMed: 23792563]
- Toledo RA, Qin Y, Cheng ZM, Gao Q, Iwata S, Silva GM, Prasad ML, Ocal IT, Rao S, Aronin N, et al. Recurrent Mutations of Chromatin-Remodeling Genes and Kinase Receptors in Pheochromocytomas and Paragangliomas. *Clin Cancer Res*. 2016; 22:2301–2310. [PubMed: 26700204]

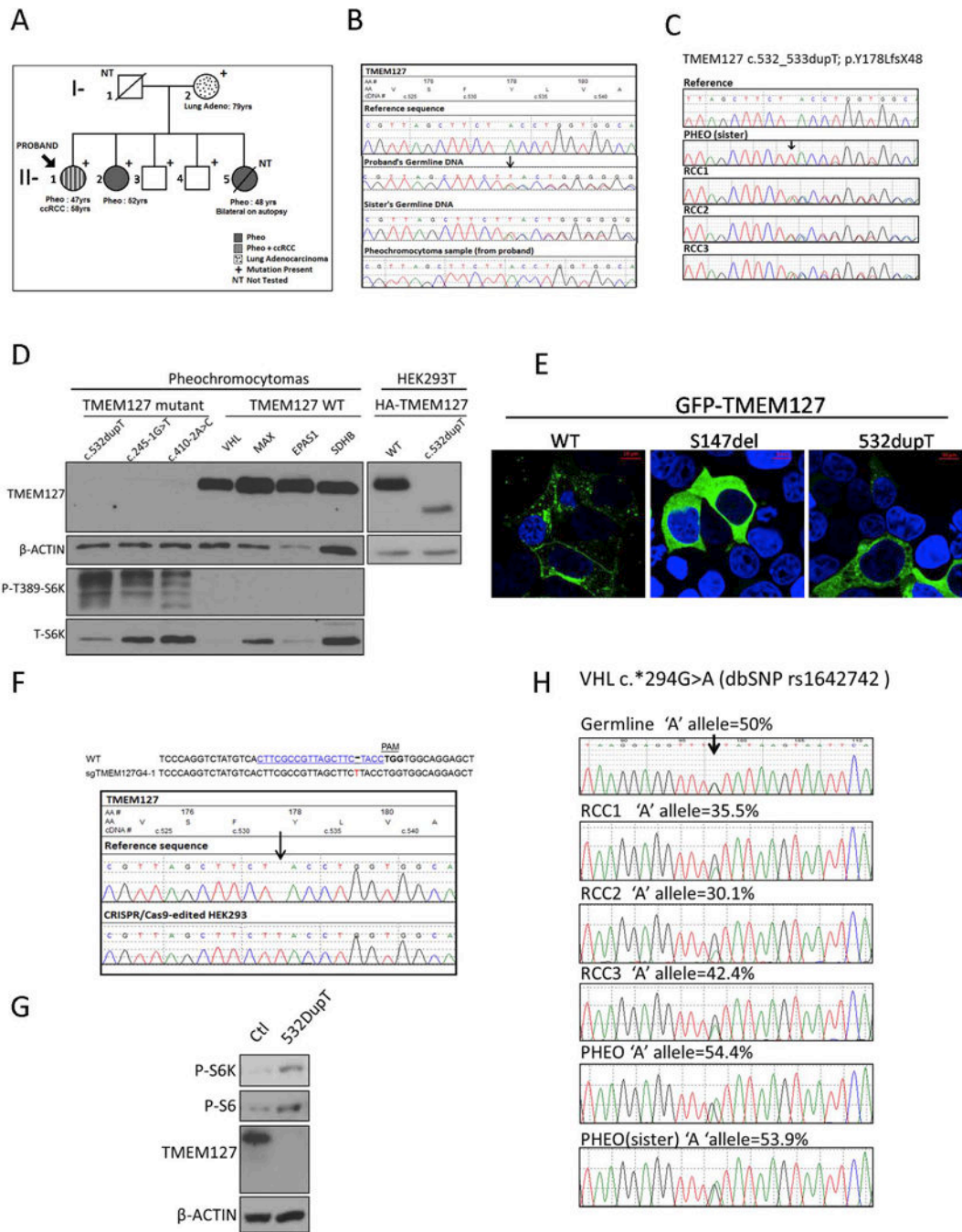


**Figure 1.**

A) Partial pedigree of a family with a germline *TMEM127* mutation (c.532dupT, p.Y178LfsX48). Clinical features are indicated in the labels. Clinically unaffected mutation carriers are 87 (I-2), 62 (II-3) and 60 (II-4) years old. One additional, 54-year-old sibling (not shown) is negative for the mutation. B) Electropherograms of germline DNA from the proband (II-1) and one affected sister (II-2), and fresh-frozen PHEO from the proband, compared to the reference sequence. The single nucleotide insertion site is indicated with an arrow; the PHEO sample has no wild-type allele sequence. C) Electropherograms of

archival, formalin-fixed and paraffin embedded tumor DNA: PHEO from affected sister and three separate subregions of the proband's RCC, referred to as RCC-1, RCC-2 and RCC-3, compared to the reference sequence. Note loss of the wild-type allele in the PHEO but not in the RCC subregions. D) Western blot of lysates from the proband's PHEO, two unrelated PHEOs carrying distinct *TMEM127* mutations, and four PHEOs of other genetic backgrounds (mutated gene indicated), a separate gel of HEK293T cells expressing wild-type or c.532dupT *TMEM127* construct containing an HA tag are shown to indicate the expected size of truncated c.532dupT *TMEM127*; Membranes were probed with *TMEM127* (Bethyl Labs), phospho-Thr389- S6 kinase (S6K) and total S6K (Cell Signaling Technology), and  $\beta$ -actin (Sigma) as a loading control. E) Confocal microscopy images of HEK293T cells transiently transfected with GFP-tagged wild-type (WT) *TMEM127* and GFP-*TMEM127*-532dupT mutant protein; a previously reported pathogenic mutant, GFP-*TMEM127*-S147del, was included as a positive control. WT-*TMEM127* has a punctate pattern, S147del is diffusely distributed, and 532dupT is predominantly diffuse. F) GuideRNA (sgRNA) sequence used to genome-edit HEK293 cells, indicating the protospacer adjacent motif (PAM) sequence and the position of the nucleotide insertion of a clone. Corresponding electropherogram is shown below (arrow indicates inserted T at position c.532 on the *TMEM127* sequence).G) Western blot of lysates from HEK293 control and 532dupT cells after amino acid starvation followed by exposure for 15 minutes. No *TMEM127* protein is detected in the HEK293-*TMEM127*-532dupT cells. Phosphorylation of mTOR targets S6 kinase (S6K) and downstream S6 are shown and  $\beta$ -actin was used as a loading control. H) Electropherograms of germline and tumor samples spanning a *VHL* 3'UTR SNP (dbSNP rs1642742) used to estimate copy number at the *VHL* gene. DNA from proband's germline and archival RCCs, as well as PHEO from proband and her sister PHEO. Percentage of the 'A' allele representation of each sample was estimated by the Mutation Surveyor program, as reported(Toledo, et al. 2016).